Capillarity

Vol. 13, No. 1, p. 10-23, 2024

Original article

Experimental and numerical study of the water-in-oil emulsions in porous media

Taha Zarin[1]*, Mohammadreza Aghajanzadeh[2], Masoud Riazi[1,3]*, Mojtaba Ghaedi[1], Mohammad Motealeh[4]

[1]*Enhanced Oil Recovery (EOR) Research Centre, School of Chemical and Petroleum Engineering, Shiraz University, Shiraz 7193616511, Iran*

[2]*Department of Civil Engineering, Monash University, Melbourne 3800, Australia*

[3]*School of Mining and Geosciences, Nazarbayev University, Astana 010000, Kazakhstan*

[4]*Iranian Offshore Oil Company (IOOC), Tehran 1966653943, Iran*

Keywords:
COMSOL Multiphysics
porous media
two-phase flow
T-junction microfluidics
water-in-oil emulsions

Cited as:
Zarin, T., Aghajanzadeh, M., Riazi, M., Ghaedi, M., Motealeh, M. Experimental and numerical study of the water-in-oil emulsions in porous media. Capillarity, 2024, 13(1): 10-23.
https://doi.org/10.46690/capi.2024.10.02

Abstract:
In different industries and environments, water-in-oil emulsions are complicated mixtures of multiple phases. They are useful for enhanced oil recovery, petroleum refining, and oil spill remediation. The behavior and properties of water-in-oil emulsions through porous media depend on several factors, such as interfacial tension, contact angle, and oil viscosity. In this work, modeling of water-in-oil emulsions was performed using COMSOL Multiphysics and validated using experimental data. The utilized experimental method included a T-junction microfluidic device to visualize and measure how the water droplets in water-in-oil emulsions differ in size, shape, and displacement. A sensitivity analysis was conducted to evaluate the impacts of interfacial tension, contact angle, oil and water channel size, and oil viscosity on the water and oil droplet sizes, distribution, and mobility in porous media. The results show the effects of water salinity, flow rates, and asphaltenes on the interfacial tension and water droplet size in water-in-oil emulsions using a T-junction microfluidic device. The size of droplets water-in-oil emulsions is influenced by the water's salinity, the interfacial tension between water and oil, and the flow rate within each phase. The optimal water droplets were obtained by the seawater diluted two times (SW#2), and the droplet shape and breakup were influenced by the shear rate, reynolds number and weber number. The rates of flow affect the shaping and division of droplets, while the suggested modeling approach can precisely depict the behavior and structure of water-in-oil emulsions within porous media. The findings of this research provide valuable insights for optimizing the performance and efficiency of water-in-oil emulsion processes.

1. Introduction

Energy is vital for human civilization, enabling various activities and processes in different sectors, such as industry, transportation, communication, and daily life. Energy can be obtained from multiple sources and types, such as renewables (hydro, wave, solar, wind, etc.), nuclear, and fossil fuels (Kousksou et al., 2014). Each source and type has its benefits and drawbacks regarding availability, cost, environmental impact, and efficiency. Fossil fuels are the most dominant source of energy in the world, as they are abundant, cheap, and easy to transport and store (Aghajanzadeh et al., 2019; Mohammadi et al., 2023). Oil production is a complex and challenging operation that involves many steps, such as drilling, casing, cementing, perforating, testing, completing, stimulating, and producing wells. Oil production also faces many problems, such as declining reservoir pressure, water invasion, gas coning, formation damage, corrosion, scaling, and environmental

Yandy Scientific Press

*Corresponding author.
E-mail address: tahazarin1452@gmail.com (T. Zarin); aghajanzadeh93@gmail.com (M. Aghajanzadeh); mriazi180@gmail.com (M. Riazi); mojtaba.ghaedi@gmail.com (M. Ghaedi); motealeh@yahoo.com (M. Motealeh).

Received May 20, 2024; revised June 14, 2024; accepted July 3, 2024; available online July 9, 2024.

issues (Aghajanzadeh and Sharifi, 2019; Zarin et al., 2023).

Water-based injection is a method of enhanced oil recovery (EOR) that involves injecting water into the reservoir to boost oil pressure and mobility. The characteristics and makeup of the utilized water can influence the process of water injection and subsequent oil production. Water injection can be classified into four types, including seawater (SW), low salinity water (LSW), smart water, and nanofluids (Yang et al., 2022; Mahmood et al., 2024). LSW injection can enhance oil production by various mechanisms, such as the movement of fine particles, the dissolution of minerals, the partial detachment of mixed-wet solids, the rise in pH level and the reduction in interfacial force, the formation and breaking of droplets, and the effect of electric charges on surfaces (Wang et al., 2022). Chemical methods can also enhance oil recovery by mobilizing the oil that is trapped in the porous media of the reservoirs (Ntente et al., 2023). Surfactants can enhance oil recovery by wettability alteration and by reducing the interfacial tension (IFT) between water and oil (Ma et al., 2022). The choice of surfactant depends on the characteristics of the reservoir rock, oil, water, and their interactions. However, surfactants may also form emulsions under certain conditions, such as the chemical characteristic of oil, the salinities of water, the type of surfactants, acidity, water-to-oil ratio, emulsion preparation method, and injection rate. An emulsion consists of two fluids that do not mix, like oil and water. Emulsions are common in various stages of oil production and processing, and three main types can be divided into water-in-oil (W/O), oil-in-water (O/W), and multiple emulsions (Yeh et al., 2023). The type of emulsion depends on various factors that affect the continuity of the phases (El-Aooiti et al., 2023). Emulsions can be used to improve oil recovery in some cases. For example, W/O emulsion can help produce heavy oil because it has a higher viscosity than crude oil. However, the viscosity rises as the amount of water dispersed in the oil phase of the emulsion increases, and the pore spaces in the reservoir may be blocked by large droplets, this can hinder oil production at high water percentages (Jiang et al., 2023; Ming et al., 2023; Liu et al., 2024). Laboratory methods are essential for the investigation and study of oil reservoirs, as they can provide valuable information about the physical and chemical properties of the reservoir rocks and fluids, the interactions between them, and the potential for EOR (Anna, 2003; Xiao et al., 2022). Laboratory methods can also help to validate and calibrate numerical models and simulations of reservoir behavior and performance. One of the laboratory methods that can be used for the study of oil reservoirs is the use of microfluidics (glass micromodels). Microfluidics involves the science and technology of controlling fluids at the microscale, and glass micromodels are microfluidic devices that are fabricated from glass and have etched or engraved patterns that mimic the pore structure and geometry of reservoir rocks. Glass micromodels can be used to visualize and quantify the fluid flow and transport phenomena in porous media, such as multiphase flow, capillary pressure, relative permeability, wettability, IFT, and displacement efficiency (Tan et al., 2004; Ward et al., 2005; Sun et al., 2021).

Bera et al. (2012) examined how oil-water microemulsions, potential candidates for EOR using microemulsion flooding, dissolve and reach equilibrium. The research team conducted a thorough search for both anionic and cationic microemulsions, aiming to identify those that demonstrate optimal performance for the intended application. They also studied how factors like salinity, the alkane carbon number, and the amount of surfactant affect the formation of microemulsions. They found that these properties are significant for preparing microemulsions for EOR. Most of the research on how emulsions flow through porous media and lower their ability to let fluids pass through has used core flooding experiments or modeling. Micromodel methods can reveal what happens to the fluids when they are pushed out, but few micromodel studies have looked at how the pores change when emulsions flow through them. Soo and Radke (1984) employed the micromodel to investigate the flow characteristics of an O/W emulsion. The flow regimes were identified by analyzing the pressure drop and oil recovery. However, they did not report any images of the pore surface events during the emulsion flow. Rezaei and Firoozabadi (2014) investigated the flooding performance of crude oil that forms stable emulsions when mixed with salt water at both micro- and macro-scale. They conducted flooding experiments in Berea cores and a glass microfluidic. They found that, due to the in-situ emulsification, a large proportion of the spaces in the glass micromodel could be blocked, during flooding, and high-pressure drops and fluctuations in pressure are resulted. They also reported some operational challenges due to the emulsion formation. Using different micromodels, Unsal et al. (2016) visualized how O/W emulsions and microemulsions form and flow. They first used a micromodel that had a matrix and a fracture to see how O/W emulsions improved oil recovery. They utilized a micromodel featuring a T-Junction to observe the formation of microemulsions and the transition of their phases. Additionally, they correlated the velocity of flow and the spontaneous emulsification rate using a micromodel equipped with dead-end pores. They discovered that when the conditions were ideal, with constant flow rate, salinity, surfactant concentration, and water-to-oil ratio, the emulsions were easy to manage and their dynamic behavior was the same as their static behavior. But, in a reservoir micromodel that simulated the EOR process, they saw phases that were not in equilibrium and water droplets in the microemulsion phase that grew bigger. They observed both types of emulsions when they used alkaline flooding in a small-scale model of a reservoir, based on these observations, they suggested a method to enhance oil extraction efficiency. Tagavifar et al. (2017) studied how microemulsions switched from balanced to unbalanced states at the pore level and assumed local balance for creating emulsions. They also linked the flow patterns of surfactant flooding to how the emulsions changed in a small-scale model with nodules made of polydimethylsiloxane. The findings highlighted the intricate changes in emulsions during chemical flooding in porous media, but they also brought up further questions about the formation and movement of complex emulsions in heavy oil reservoirs.

Previous research has used various physical geometries to form and control emulsion droplets, such as the T-junction

framework (Guillot and Colin, 2005; Gupta and Kumar, 2010; Kovalchuk and Simmons, 2023), flow-focusing arrangements (Romero and Abate, 2012; Ho et al., 2022; Kim et al., 2022), and co-flowing geometries (Cramer et al., 2004; Battat et al., 2022). Thorsen et al. (2001) were the first researchers that use T-junction microarrays. In their study, they formed water droplets by slow flow under two different mechanisms of surface tension and shear stress. However, recent studies on T-junction micromodels have shown that various factors, such as the flow rate of continuous and dispersed fluids, the relative viscosity of liquids (Sattari et al., 2020), and the size of microfluidic channels (Garstecki et al., 2006), can influence the droplet shape. He et al. (2022) concluded that the flow pattern in the microfluidic T-junction changes when the dispersed phase velocity increases. Also, various models were used to model the behavior of the formed drops, such as the fuzzy field method model, the level set method (LSM), the Boltzmann network method, the volume of fluid (VOF) method, etc. Sang et al. (2009) studied the effect of viscosity on the formation or deformation of droplets in a microfluidic T-junction with two VOF methods and the Lattice Boltzmann method. They found similar results and noted that the droplet shape remained unchanged after reaching a contact angle of 165°. De Menech (2006) simulated how droplets were formed at microfluidic T-junction using the phase field method. The LSM is a different method that can handle both flow phases, compressible and incompressible, and can show the interface with a smooth shape. It is less affected by the interface thickness parameter, enhancing accuracy and reducing computational costs compared to the phase field method and implementation is generally more straightforward and computationally efficient for accurately capturing the interface (Persson, 2013). This method allows for finer control over the interface's movement, particularly when dealing with complex or variable velocity fields (Osher and Fedkiw, 2001; Boniou et al., 2022). Thai et al. (2018) used the LSM to model a T-junction environment with a two-phase and laminar flow from a contact angle of 135°. They studied the effect of injection flows on droplet formation. They found that the size of the dispersed fluid droplets had a linear relationship with the injection flow rates of the continuous fluid and an exponential relationship with the injection flow rates of the dispersed fluid.

Water injection is a common method of EOR from reservoirs, as mentioned earlier. However, water injection can cause various problems, such as mineral and organic scaling, and undesirable emulsification, because of the interaction between the reservoir fluids and injected water. Hence, examining the emulsion resulting from the interaction between water and oil in the reservoir is essential. The emulsion can affect the oil recovery in different ways, depending on its type and stability. For example, a W/O emulsion can increase the oil viscosity, especially in heavy oil reservoirs, and block the pore spaces in the reservoir by large droplets as the water content increases. This can hinder oil production at high water percentages. On the other hand, an unstable emulsion that separates quickly can reduce the efficiency of the water injection process. The formation of W/O emulsions is one of the challenges faced by the oil and gas industry, which can also cause pressure fluctuations and operational difficulties for refineries and petrochemicals (Duraiswamy and Khan, 2009; Zhang et al., 2024).

This research aims to examine the water injection control process by observing and analyzing the emulsion injection in the reservoir. The emulsion formation can lead to an additional pressure differential around the wellbore area, resulting in a reduction in the well production rate. Thus, examining the behavior and stability of the emulsion is crucial. To accomplish this, micromodels were utilized as a tool to observe the processes within porous media accurately. The proposed method uses COMSOL Multiphysics software, which is a powerful and valuable tool for Multiphysics modeling and simulation. The method is validated using experimental data obtained from a T-junction microfluidic device, a simple and effective device for generating and controlling emulsion droplets. The proposed method is also necessary because it can provide valuable information and guidance for designing and optimizing EOR processes using W/O emulsions. To the best of our knowledge, this is one of the few attempts in recent years to combine LSM and VOF methods for modeling emulsion and flow in porous media. The numerical simulations demonstrate strong alignment with the experimental data. This research investigates the interaction of water-based fluids and oil in forming water droplets under different conditions. Previous studies did not thoroughly examine the effective parameters of the water droplet formation process and their stability. They often presented either modeling or experimental results separately. This study however compares both experimental and modeling results and performs sensitivity analysis on some effective parameters of the droplet formation process and their stability.

2. Methodology

The methodology of this work consists of two main parts: experimental and modeling. The experimental part uses a T-junction microfluidic device to generate W/O emulsions under different conditions. The modeling part uses COMSOL Multiphysics software to simulate the emulsion formation, behavior, stability, and flow in porous media. The software is a powerful Multiphysics modeling tool, that can handle complex geometries, boundary conditions, and coupled phenomena.

2.1 Experimental

The experimental data validate the numerical simulations and assess the impact of various parameters on emulsion behavior and oil production.

2.1.1 Crude oil

Crude oil from an offshore reservoir in the south of Iran was used in this study. The quality and production of crude oil depend on its properties, such as viscosity, density, TAN (Total Acid Number), TBN (Total Base Number), and API gravity. Table 1 shows the characteristics of the crude oil in this research.

Table 1. Crude oil properties.

Property	Value
Viscosity (cP)	8.3
Density (g/cc)	0.85
API (-)	35.4
TAN (mgKOH/g)	0.15
TBN (mgKOH/g)	1.52

Table 2. Ionic analysis of SW.

Ion type	Value (mg/L)
Na^+	17,412
K^+	0
Ca^{2+}	240
Mg^{2+}	2,488
Cl^-	21,493
SO_4^{2-}	3,247
$NaHCO_3^-$	1,120
TDS	46,000

Table 3. Selected brine samples.

Brine sample	Salinity (ppm)
SW	46,000
SW#2	23,000
SW#5	9,200
SW#10	4,600

2.1.2 Brine

The artificial SW was prepared based on the ion analysis of Persian Gulf Sea Water, which had a total dissolved solids (TDS) of 46,000 ppm based on the ionic chromatography according to Table 2. LSW diluted two, five, and ten times from the SW were also used. These experimental groups had salinities of 46,000, 23,000, 9,200, and 4,600 ppm, respectively according to Table 3.

2.1.3 Micromodel fabrication

The following steps were used to make glass micromodels. First, two pieces of glass with the same thickness and size were taken. They were washed and dried, and then one of them was covered entirely with colored adhesives that were resistant to acid treatment. Next, the design of the model was crafted using Corel Draw software, selected specifically for its vector imaging capabilities. This feature ensures that image and pattern quality remain intact, even under high levels of magnification. A laser device with 100 microns accuracy was used to implement the design on the glass. The glass was etched with the desired depth using fluoric acid (HF 40%). After each use of acid, the remaining acid was removed using high-pressure water. This acid-water process was repeated three times. After drying and washing with distilled water, the glass was ready for drilling and installing the input and output needles. The sides of the micromodel were fixed with glue. The final step involved placing the micromodel in an electric furnace and heating it to 700 °C to ensure complete attachment of both glasses. Fig. 1 shows the schematic pattern of microfluidic T-junction. The width of the continuous (oil) and dispersed fluid (water) channels is 100 μm.

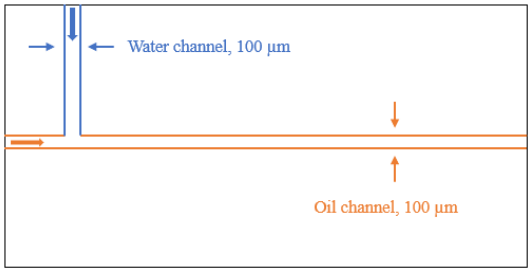

Fig. 1. Schematic of microfluidic T-junction pattern.

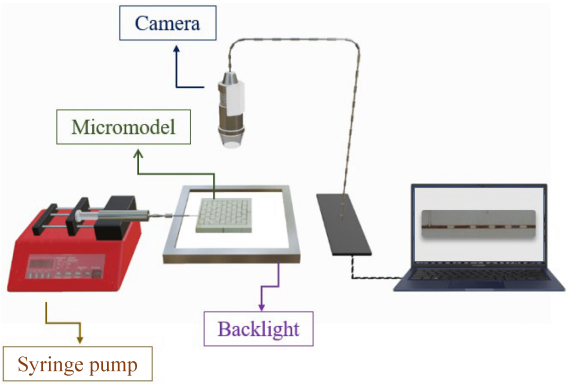

Fig. 2. Schematic of the microfluidic experimental setup.

2.1.4 Microfluidic set-up

The laboratory setup shown in Fig. 2 was used to perform dynamic tests. This setup consisted of a horizontal glass micromodel, a backlight, a syringe pump (To optimize the flow rate, place two pumps perpendicular to the injection lines), and a microscopic camera (AM4112T Dino-Lite). Oil and water-based fluids were injected into the microfluidic, and their interaction was recorded with the camera.

2.1.5 IFT measurement

A device from the Kruss company (DSA 100) was utilized to measure the static IFT at ambient temperature and pressure. This device had a lifter, an injection chamber for the syringe, and a base for holding the saline chamber (Salehpour et al., 2021). The device functioned by introducing a drop of oil in a specific volume of brine (a tiny quartz container) and using a fixed rate in microliters. The taken images were analyzed with ImageJ software and IFT for all tests was measured.

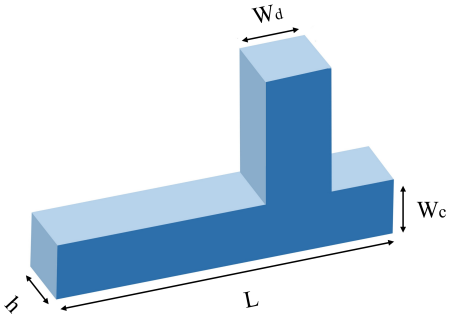

Fig. 3. Schematic of three-dimensional T-Junction micromodel.

Table 4. Physical dimensions of T-Junction micromodel.

Geometry	W_c	W_d	h	L
Value (μm)	100	100	25	40,000

Table 5. Properties used in COMSOL software to build a basic model based on laboratory results.

Property	Value	Continuous fluid (Oil)	Dispersed fluid (Brine)
IFT (mN/m)	16.4	/	/
Contact angle (θ_w)	120	/	/
Density (Kg/m^3)	/	0.85	1.01
Dynamic viscosity (cP)	/	8.3	1
Flow rate (mL/hr)	/	1	1
Channel size (μm)	/	100	100

2.2 Modeling

Fig. 3 shows the schematic of the three-dimensional T-junction micromodel. This micromodel consists of two perpendicular channels: A horizontal channel for the oil flow and a vertical channel for the water-base fluid flow. The horizontal channel size is W_c and the vertical channel size is W_d. The depth of both channels is equal to each other (h) and the length of the horizontal channel is L. The governing equations required to simulate fluid dynamics in the environment of the T-junction in Fig. 3 are Navier-Stokes, Continuity, and Level Set shown in Eqs. (1)-(3), respectively:

$$\rho\frac{\partial u}{\partial t}+\rho\left(u\cdot\nabla\right)u=\nabla\cdot\left[-pI+\mu(\nabla u+(\nabla u)^T)\right]+F_{st} \quad (1)$$

$$\nabla\cdot u=0 \quad (2)$$

$$\frac{\partial\phi}{\partial t}+u\cdot\nabla\phi=\gamma\nabla\cdot\left[-\phi\left(1-\phi\right)\frac{\nabla\phi}{|\nabla\phi|}+\varepsilon\nabla\phi\right] \quad (3)$$

where ρ is the density (kg/m^3), u is the velocity (m/s), t stands as time (s), p stands as pressure (Pa), I is the identity matrix, μ is dynamic viscosity (Pa·s), T is temperature (°C) and F_{st} stands as the IFT force that enters the interface between two fluids (N/m^3). γ and ε are numbers that help to stabilize the calculations. The parameter ε, which controls the interface thickness, is a constant value throughout the domain. The parameter γ is for reinitializing the level set function and maintaining a constant interface thickness. ϕ represents a scalar function that defines the level sets of a domain. The dynamical viscosity is given by the following equations:

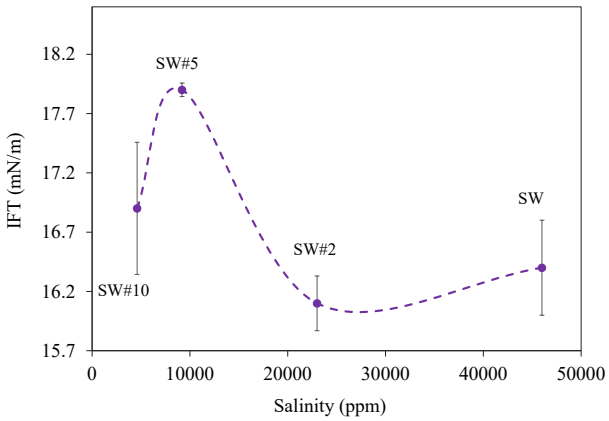

Fig. 4. IFT results.

$$\rho=\rho_1+(\rho_2-\rho_1)\phi \quad (4)$$

$$\mu=\mu_1+(\mu_2-\mu_1)\phi \quad (5)$$

where in this study water is represented by 1, and oil is represented by 2.

Eq. (6) shows how the density and viscosity of both fluids 1 and 2 were set and changed. The fluid flows smoothly from the right side. This model does not have any stress. The wall type is a boundary that is wet by the fluid. The following expression can be used to find the effective diameter of a droplet:

$$d_{eff}=2\sqrt[3]{\frac{3}{4\pi}\int_{\Omega}^{\infty}(\phi>0.5)\mathrm{d}\Omega} \quad (6)$$

where the effective diameter of the droplet is d_{eff}, and Ω stands for the horizontal channel leftmost part (Van der Graaf et al., 2006).

The dimensions of the microfluidic T-junctions were meticulously selected based on a comprehensive review of previous research and the practical constraints imposed by our laboratory's fabrication capabilities (Garstecki et al., 2006; Xu et al., 2006; Hoang et al., 2013; Unsal et al., 2016; Thai et al., 2018). Table 4 shows the physical dimensions of the T-Junction micromodel, and Table 5 shows the properties used in COMSOL software to build a basic model based on laboratory results.

3. Results and discussion

The results of the IFT measurements and T-junction micromodel studies are presented in this section. The validation of the results shows the comparison between experimental tests with modeling. A sensitivity analysis is conducted using the developed model to assess the impact of various parameters on fluid displacement.

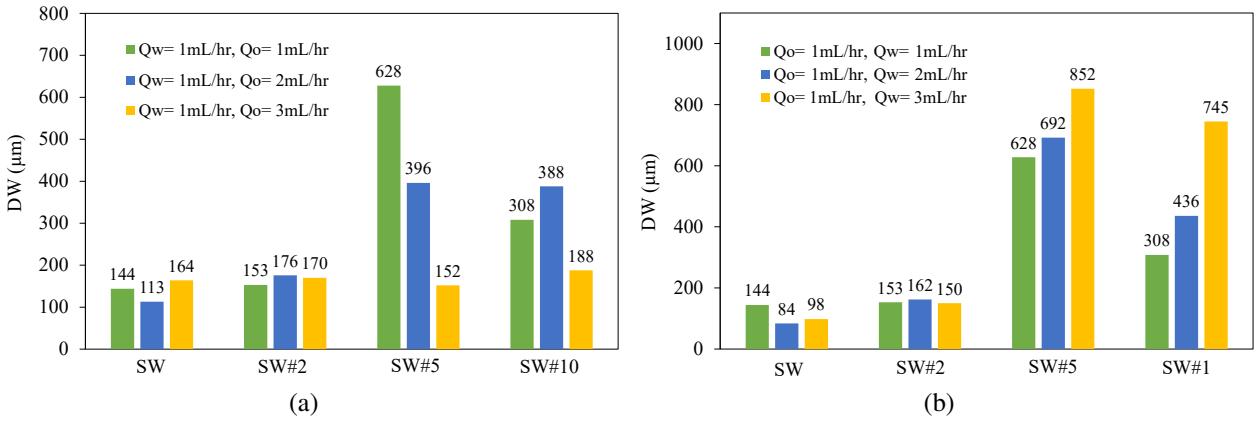

Fig. 5. Water droplet size of LSW by: (a) Constant Q_O and (b) constant Q_w.

3.1 IFT results

Fig. 4 presents the IFT results between oil and brine at various salinities. The IFT behavior can be categorized into two regions: In the first region, the IFT increases as the salinity decreases, and in the second region, the IFT decreases as the salinity decreases. This non-uniform behavior can be explained by the effects of salt, polar components, and surfactants at the oil-water interface. The IFT between oil and brine depends on the salinity and acidity of crude oil, as well as the surface behavior of crude oil components, which is more complex than pure systems. Salinity affects the IFT by changing the structure and energy of water and salt bonds. When the hydrocarbon phase is present, the salt ions migrate from the interface to the bulk phase of the brine, creating a negative surface energy for the salts. This migration increases the IFT. Therefore, higher salinity leads to higher IFT. However, this effect can be disrupted by the presence of surfactants, like asphaltenes. Asphaltenes are molecules with both hydrophilic and hydrophobic groups, and they typically gather at the oil-water interface. This makes the system more thermodynamically stable and reduces the IFT. Therefore, lower salinity leads to lower IFT. However, this effect is only dominant before a salinity threshold value. After that, the effect of salt becomes more substantial than the effect of asphaltene, and the IFT increases again as the salinity decreases. This phenomenon is known as salting-in and salting-out effects. The optimal point with the lowest IFT is determined by the competition between asphaltene and salt for controlling the oil-water interface (Doryani et al., 2018; Rahimi et al., 2020; Tangparitkul et al., 2023).

3.2 Experimental results of T-junction micromodel

Fig. 5 shows the average size of W/O emulsion droplets for different LSW and different oil and water injection flow rates. The water droplets are the largest for the seawater diluted five times (SW#5), consistent with the IFT results. The SW#5 had the highest IFT, which means that the water droplets were more resistant to deformation and breakup. This can be seen in Fig. 4, where the IFT values for different salinities are plotted. The flow rate of both the continuous and dispersed phases also plays a role in droplet size. The water droplets increase in length as the injection rate increases to a constant oil flow. The water droplets are smaller when the oil injection rate increases at constant water flow rates. This trend is in agreement with similar studies (Garstecki et al., 2006).

Eqs. (7)-(9) present the formulas for calculating the capillary, reynolds and weber dimensionless numbers, respectively. The capillary number (Ca) is defined as the ratio of viscous forces to surface tension forces, The reynolds number (Re) quantifies the relative significance of inertial forces over viscous forces. Lastly, the weber number (We) compares the inertial forces to the surface tension forces. In these equations, σ is surface tension (Zhang et al., 2017; Yi et al., 2022):

$$\mathrm{Ca} = \frac{u\mu}{\sigma} \tag{7}$$

$$\mathrm{Re} = \frac{\rho u L}{\mu} \tag{8}$$

$$\mathrm{We} = \frac{u}{\sqrt{\frac{\sigma}{\rho L}}} \tag{9}$$

After diluting the brines, the Ca which measures the strength of the fluid's thickness against the force that holds droplets together is expected to go up. This happens because the fluid gets thinner and might flow faster. When the Ca gets higher, it means the fluid's thickness plays a bigger role than the droplet-holding force, making the droplets grow bigger, take on irregular shapes, and break apart more easily. The Re which tells us if the flow is laminar or turbulent is expected to go up. This is because the fluid becomes less viscous and might move faster. A bigger Re means there's a greater chance for the flow to be chaotic, which can make the droplets form in more uneven shapes and split apart more easily. Similarly, the We might rise too if the fluid starts moving faster after being diluted, even though the fluid itself is lighter (less dense). The We helps us understand if the force of the fluid's movement (inertia) is stronger than the force that keeps the droplet together (surface tension). When the We gets bigger, it shows that the movement force is winning, making the

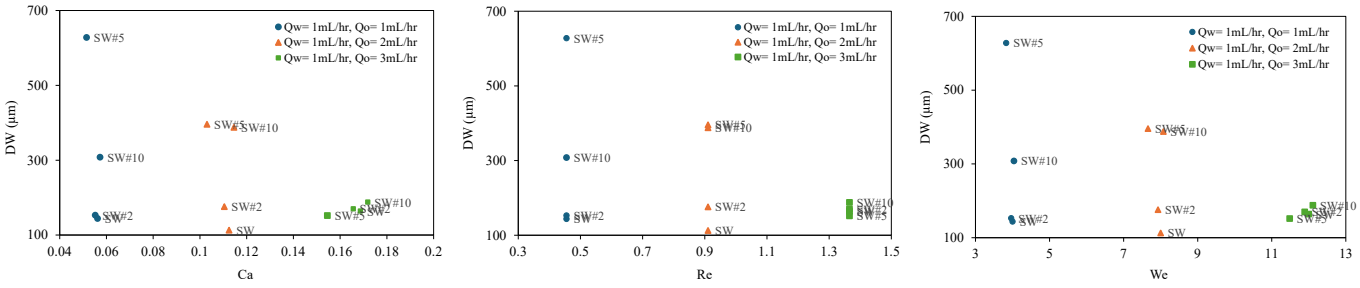

Fig. 6. Water droplet size of LSW vs. (a) Ca, (b) Re and (c) We at different Q_O.

Fig. 7. The effect of water injection rate on the shape and size of water droplets in experimental tests Q_O = 1mL/hr and Q_W: (a) 1 mL/hr, (b) 2 mL/hr and (c) 3 mL/hr.

droplets stretch out more and break apart more readily (Jang et al., 2019; Shende et al., 2021; Lv et al., 2023).

Fig. 6 presents a series of graphs illustrating the influence of dynamic fluid parameters on droplet size within a W/O emulsion. Specifically: Fig. 6(a) delineates how varying Ca correlates with droplet size across distinct batches of LSW, each subjected to different oil injection rates. Fig. 6(b) depicts the relationship between Re and droplet size for these groups, again considering the variation in oil injection rates. Fig. 6(c) charts the droplet size as a function of We, providing insights into the interplay between inertial and surface tension forces under diverse conditions of salinity and injection rates. The injection rate directly affects the characteristic velocity in the formulas for the Ca, Re and We. An increase in injection rate typically leads to a higher velocity, which can result in smaller droplet sizes due to increased shear forces overcoming the surface tension. Conversely, a lower injection rate may lead to larger droplets as the kinetic energy is insufficient to surpass the surface tension forces. In the context of the Re, a higher injection rate implies a higher velocity, which can indicate a transition from laminar to turbulent flow, affecting the droplet formation process (Li et al., 2023).

Fig. 7 shows how the water injection speed for seawater diluted two times (SW#2) affects the shape and size of water droplets in the experimental tests. This experiment examines how the structure and shape of water droplets in W/O emulsion are affected by the water injection flow rate. The water and oil were injected at the same flow rate of 1 ml/hr initially, and then the water flow rate was increased to 2 and 3 ml/hr subsequently. The changes in the water droplet size and morphology were observed and recorded. The results show that both the water and oil flow rates have an impact on droplet size. With increasing water flow rates, the droplet size will increase but decrease with increased oil flow rates. This can be explained by the effects of shear rate, Re and We on the droplet deformation and breakup processes. The shear rate is how fast the velocity changes when one layer of fluid moves over another layer. The Re measures how much the fluid's momentum and friction affect its flow. We measure how much the fluid's momentum and surface tension affect its flow (Mangani et al., 2022). These dimensionless numbers describe the relative significance of various forces acting on the droplets. The shear rate and the Re of water phases shall increase with an increasing water flow rate, at constant oil flow rates. This means that the water droplets experience more deformation and fragmentation caused by increased velocity gradient and inertia of the water phase. This results in larger water droplets and smaller oil droplets. However, when the oil flow rate increases at a constant water flow rate, the shear rate and the Re of the oil phase increase. This signifies that the oil droplets experience more deformation and breakup resulting from increased velocity gradient and inertia of the oil phase. This results in smaller water droplets and larger oil droplets. We also affect the droplet size by influencing the IFT. The IFT is the force per unit length that acts on a line drawn on the interface between two immiscible fluids like oil and water. The IFT tends to minimize the surface area of the droplets and resist their coalescence and coarsening. The We of the water phase is increased when the water flow rate rises at an unchanging oil flow rate. This indicates that the inertial forces overcome the interfacial forces and cause more coalescence and coarsening of the water droplets. This also results in larger water droplets and smaller oil droplets. However, the We of the oil phase increases as the oil flow rate is increased to a steady water flow rate. This represents that the inertial forces overcome the interfacial forces and cause more coalescence and coarsening of the oil droplets. This also results in smaller water droplets and larger oil droplets. Consequently, it can be concluded that the size of water droplets in W/O emulsions is influenced significantly by both oil and water flow rates. Th-

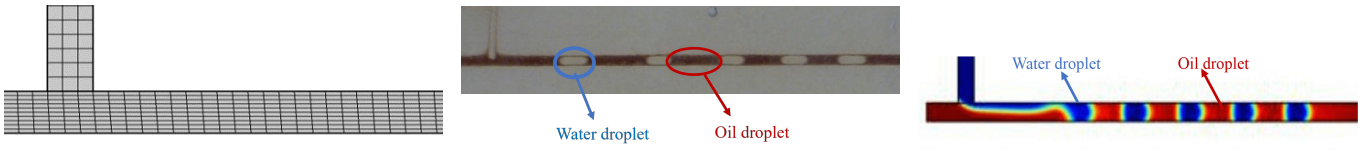

(a) (b) (c)

Fig. 8. (a) Meshed geometry for a validation model, comparison of the results obtained from (b) experimental tests and (c) modeling of COMSOL software based on the basic model with the properties of Tables 5 and 6.

Table 6. Meshing parameters used in the modeling section.

Property	Value
Maximum mesh element size (mm)	0.0342
Minimum mesh element size (mm)	1.02E-4
Maximum element growth rate	1.05
Curvature factor	0.2
Narrow regions resolution	1
Element distribution fixed number	10

Table 7. The spectrum of parameter values utilized in the sensitivity analysis.

Parameter	Range of values
IFT (mN/m)	1, 5, 10, 16.4, 20, 25
Contact angle (°)	30, 60, 90, 120, 150
Oil viscosity (cP)	1, 8.3, 30, 70, 110, 180
Oil channel size (μm)	50, 100, 200
Water channel size (μm)	50, 100, 200

ese effects are related to the balance between viscous, inertial, and interfacial forces that act on the droplets (Yi et al., 2022).

3.3 Validation results

To verify the precision of the outcomes, a comparative analysis was conducted between the experimental data and the model's forecasts. The analysis revealed a strong concordance, affirming both the model's accuracy and its dependability. A microfluidic T-junction was used to inject oil (continuous fluid) and SW (dispersed fluid) at a fixed flow rate of 1mL/hr. The experimental and simulation results were then compared with the help of COMSOL software. Fig. 8(a) the mesh distribution within the enhanced model, which has been constructed and refined according to the basic laboratory's model, is depicted, Figs. 8(b) and 8(c) compare the laboratory result and the modeling result. The average droplet size was 102 μm for the experiment and 108 μm for the simulation, which indicates a good agreement between the results. The validation of the COMSOL model was characterized by a meticulous calibration of simulation parameters to mirror realistic conditions. The relative repair tolerance was set at 1E-6, which ensured a high precision in the results. Laminar two-phase flow was simulated under a standard reference pressure level of 1 atm. The mobility tuning parameter was adjusted to 1m·s/kg to depict fluid mobility accurately. At 0.01 j/m^3, the Phi-derivative of external free energy was established, contributing to the phase interface's stability. To simulate the conditions, a wetted wall boundary was used due to the interaction between the fluid and the container walls, in conjunction with a pressure-no viscous stress boundary condition to negate shear stress effects at the boundaries. The meshing was finely tuned, with a maximum mesh element size of 0.0342 mm and a minimum mesh element size of 1.02E-4 mm, allowing for a detailed geometrical representation. The maximum element growth rate was maintained at 1.05, with a curvature factor of 0.2, ensuring smooth adaptation of the mesh to the geometry's curves. The resolution of narrow regions was kept at 1 to accurately capture the flow dynamics in smaller spaces. A fixed number of element distribution was employed, with the number of elements set to 10, to ensure uniformity across the computational domain. Such a rigorous setup of the COMSOL model parameters is foundational to the reliability of the simulation results. Detailed fluid specifications, along with the geometric layout and meshing parameters, are comprehensively presented in Tables 5 and 6, respectively.

3.4 Sensitivity analysis

Considering that the model agreed with the results of the experiments results, the sensitivity analysis was conducted using the model to investigate the effects of different parameters on the fluid displacement. These parameters include IFT, contact angle (wettability), continuous fluid (oil) viscosity, and channel size. Table 7 presents the range of values for each parameter that was varied in the sensitivity analysis. The sensitivity analysis was performed to evaluate how the fluid displacement behavior is affected by changes in these parameters.

3.4.1 IFT

Since the IFT shows the degree of repulsion between two fluids, as shown in Fig. 9, a lower value suggests complete mixing of the two fluids. As this parameter increases, the miscibility decreases, leading to subsequent stages, such as droplet formation, their growth, and eventually formation upon entering the main path. Generally, the experiments show that the force between the interfaces affects the formation of droplets; more salinity makes the droplets bigger and slower to form. An essential factor influencing the stability and rheology of the emulsions examines how IFT influences the size of wa-

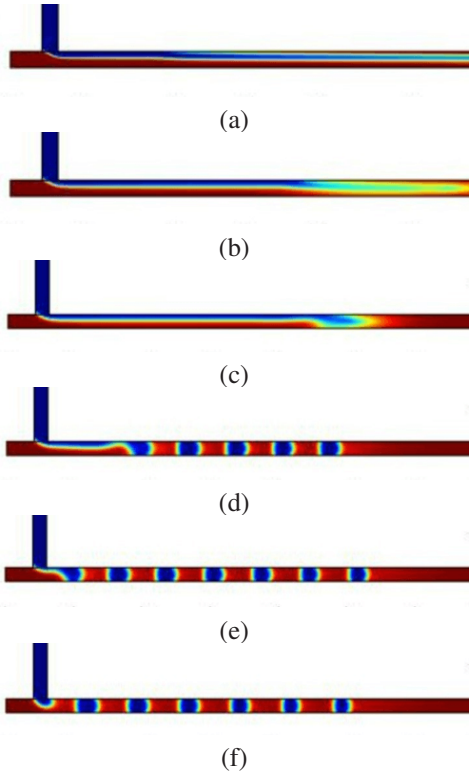

Fig. 9. The effect of IFT on the shape, number, and dynamic behavior of water droplets, (a) 1, (b) 5, (c) 10, (d) 16.4, (e) 20 and (f) 25 mN/m.

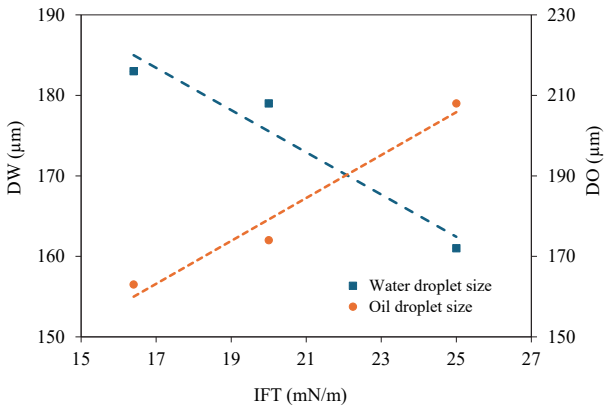

Fig. 10. The size values of water and oil droplets according to changes in IFT.

ter droplets in W/O emulsions. Generally, a higher IFT leads to larger droplet sizes, and a lower IFT leads to smaller droplet sizes. This is because the energy needed to make a new surface area between the two phases is the IFT, and smaller droplets have more surface area for each unit of volume than larger droplets. Therefore, smaller droplets are energetically less favorable than larger droplets when the IFT is high, and vice versa when the IFT is low.

In Fig. 10, the graph shows the water droplet size and oil droplet size at various IFTs, as per the modeling results. Microfluidic devices can generate monodisperse droplets of controlled size and shape by forcing a dispersed phase (water)

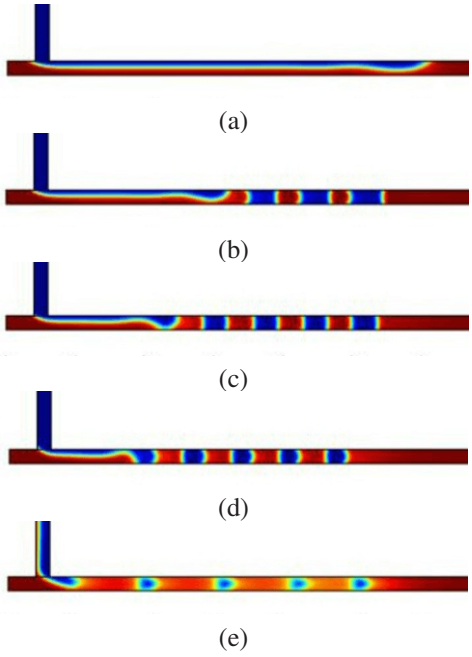

Fig. 11. The effect of contact angle (wettability) on the shape, number, and dynamic behavior of water droplets, (a) 30°, (b) 60°, (c) 90°, (d) 120° and (e) 150°.

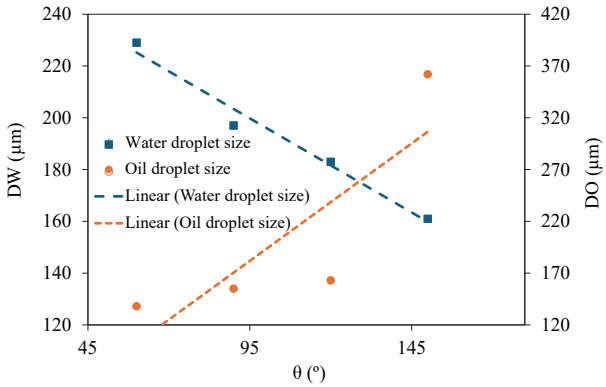

Fig. 12. The size values of water and oil droplets according to changes in contact angles.

droplets have a specific size because of the balance between the forces that make them stretch (viscous forces) and the forces that drive the droplets shrink their surface area (interfacial forces).

3.4.2 Contact angle (wettability)

According to Fig. 11, in the beginning, when the contact angle is low (i.e., strongly water-wet), no drop is formed. Then, the formation of droplets and the change in the shape of the droplets are accompanied by an increase in wettability. Finally, when the environment becomes completely oil-wetted, the concentration and size of water droplets decrease. A lower contact angle promotes wall-wetting, leading to larger water droplets by reducing surface tension between the water and the wall. Conversely, a higher contact angle inhibits wall-wetting, resulting in smaller droplets due to increased surface tension (Wang et al., 2018).

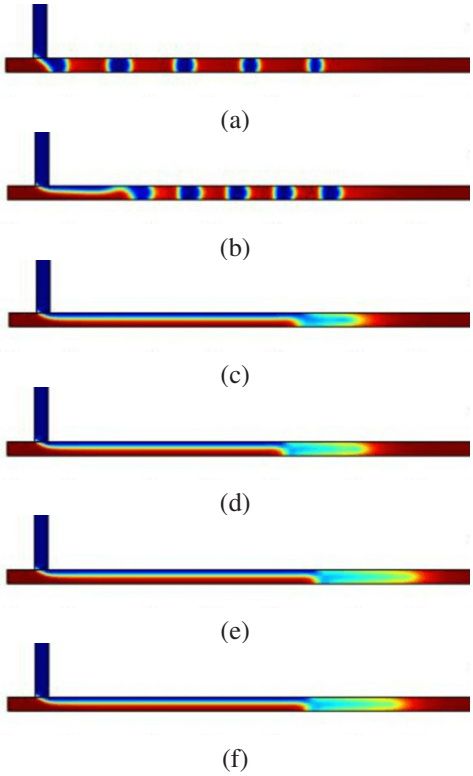

Fig. 13. The effect of continuous fluid (oil) viscosity on the shape, number and dynamic behavior of water droplets, (a) 1, (b) 8.3, (c) 30, (d) 70, (e) 110 and (f) 180 cP.

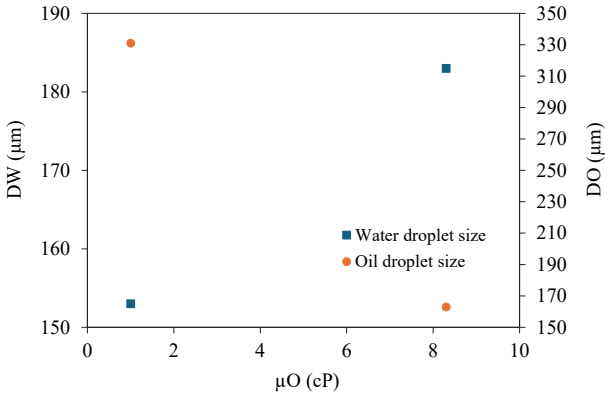

Fig. 14. The size values of water and oil droplets according to changes in oil viscosities.

In Fig. 12, the graph shows the water droplet size and oil droplet size at various contact angles, as per the modeling results. The contact angle also affects the stability and rheology of the emulsions. A lower contact angle leads to larger droplets, which increase the effective viscosity of the emulsion and make it more prone to coalescence. A higher contact angle leads to smaller water droplets, which reduce the effective viscosity of the emulsion, enhancing its stability.

3.4.3 Continuous fluid (oil) viscosity

Fig. 13 shows that as the oil viscosity increased to match the study's oil viscosity, droplet formation was observed. With further increases in oil viscosity, water continuously flowed through the oil path due to its lower viscosity. The size of water droplets in W/O emulsions is influenced by the balance between viscous and interfacial forces. The oil viscosity affects the viscous forces that elongate the droplets and resist their deformation and breakup. Interfacial forces, which tend to reduce the surface area of the droplets and prevent their coalescence and degradation, are involved in the IFT. Generally, a higher oil viscosity leads to larger droplet sizes, and a lower oil viscosity leads to smaller droplet sizes. A higher oil viscosity increases the resistance to droplet deformation and breakup, while a lower oil viscosity facilitates droplet deformation and breakup.

The graph shows the size of the water droplet and the size of the oil droplet at different oil viscosities, according to the modeling results, in Fig. 14. The effective viscosity of W/O emulsions is also influenced by the IFT and droplet size, defined as the ratio of the shear stress to the shear rate of the emulsion, it reflects how easily the emulsion can flow under an applied force (Sang et al., 2009; Yi et al., 2022). The effective viscosity is influenced by many factors, such as the volume fraction, droplet size distribution, shape, and deformation of droplets, along with both phase's viscosity ratio and rheology. Generally, a higher volume fraction, a larger droplet size, a more polydisperse size distribution, a more spherical shape, and a higher viscosity ratio led to a higher effective viscosity. The IFT affects the effective viscosity indirectly by influencing the droplet size and shape. A higher IFT tends to make larger and more spherical droplets, which increase the effective viscosity. A lower IFT tends to produce smaller and more deformed droplets, which decrease the effective viscosity.

3.4.4 Channel size

The effect of oil channel size on the water droplet size in W/O emulsions is related to the hydrodynamic conditions of the flow that generates the emulsions. The oil channel size determines the characteristic length scale of the flow, which influences the shear rate, the Re, and the We of the flow. These dimensionless numbers characterize the relative importance of different forces acting on the droplets, such as viscous, inertial, and interfacial pressures. In W/O emulsions, the size of the water droplets diminishes as the dimensions of the oil channels are reduced, provided that the flow rate and IFT remain constant. A smaller oil channel size implies a higher shear rate and a higher Re of the flow, which enhances the droplet deformation and breakup processes. A smaller oil channel size also indicates a lower We of the flow, which reduces the droplet coalescence and coarsening processes. Therefore, the formation of smaller and more stable droplets in W/O emulsions is supported by a smaller oil channel size (Gong and Towner, 2001). However, the effect of oil channel size on the water droplet size in W/O emulsions is not linear or monotonic. There is a critical oil channel size below which the water droplet size does not decrease further but increases slightly (Nguyen et al., 2013). When the oil channel size becomes too small, the flow becomes laminar and the turbulent fluctuations that contribute to droplet breakup are suppressed. Moreover, when the oil channel size becomes comparable to the water droplet size, the confinement effects become signifi-

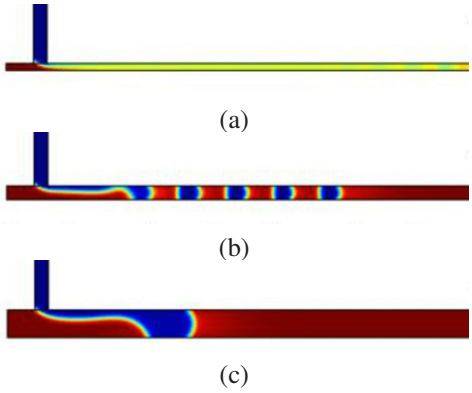

Fig. 15. The effect of oil pore size on the shape, number, and dynamic behavior of water droplets, (a) 50, (b) 100 and (c) 200 μm.

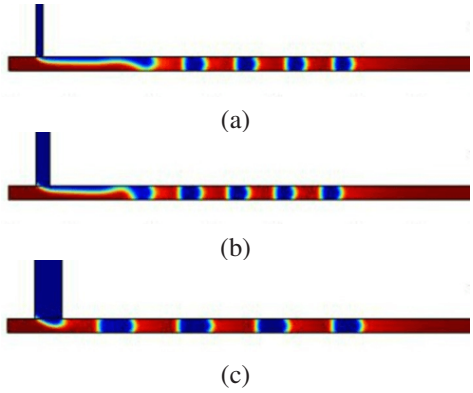

Fig. 17. The effect of Water pore size on the shape, number, and dynamic behavior of water droplets, (a) 50, (b) 100 and (c) 200 μm.

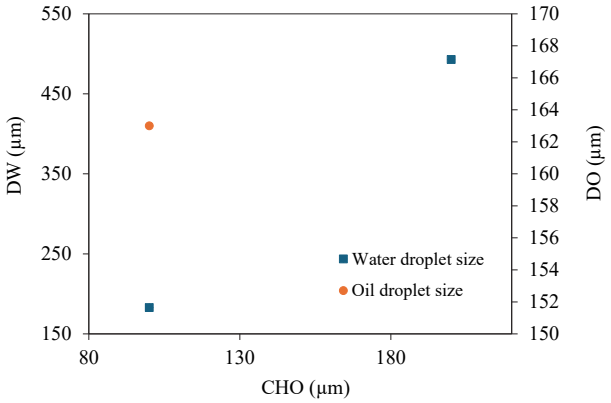

Fig. 16. The size values of water and oil droplets according to changes in oil channeling sizes.

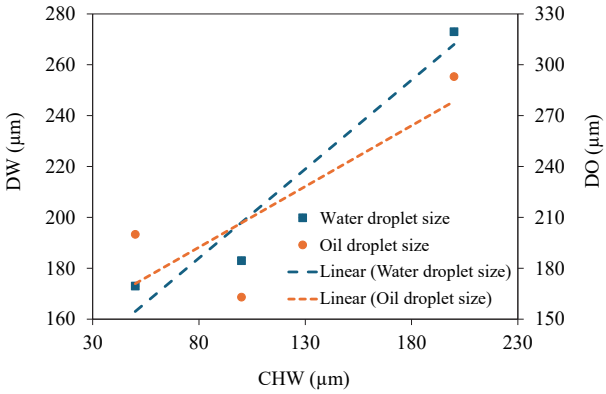

Fig. 18. The size values of water and oil droplets according to changes in water channeling sizes.

cant and the droplets tend to align with the flow direction, reducing their deformation and breakup. The typical oil channel size used in W/O emulsion studies is between 10 and 1,000 μm (Yi et al., 2022). When the oil channel size becomes larger than 1,000 μm, the flow becomes more turbulent and chaotic, and other factors such as contact angle and surfactant concentration may become more important than oil channel size in determining the water droplet size in W/O emulsions. Water droplets are formed later and need more time to reach a stable state, as shown in Fig. 15 with an increase in the diameter of the oil pore size. While decreasing the width of the side channel increases the droplet velocity, the droplet velocity is linearly dependent on the dispersed phase flow velocity. Therefore, it is easy to obtain the normal oil-water flow patterns by changing the two-phase flow rate.

The characteristic length scale of the flow, which influences the shear rate, Re, and We of the flow, is determined by the size of the water channel. These dimensionless numbers characterize the relative importance of different forces acting on the droplets, such as viscous, inertial, and interfacial forces. The water droplet size in W/O emulsions decreases with decreasing water channel size for a fixed flow rate and IFT (Yi et al., 2022). A smaller water channel size implies a higher shear rate and a higher Re of the flow, which enhances the droplet deformation and breakup processes. A smaller water channel size also indicates a lower We of the flow, which reduces the droplet coalescence and coarsening processes. Therefore, the formation of smaller and more stable droplets in W/O emulsions is influenced by a smaller water channel size. However, there is no linear or monotonic effect of the size of the water channel on the size of the water droplets in W/O emulsions. There is a critical water channel size below which the water droplet size does not decrease further but increases slightly. When the water channel size becomes too small, the flow becomes laminar, and the turbulent fluctuations contributing to droplet breakup are suppressed. Moreover, when the water channel size becomes comparable to the water droplet size, the confinement effects become significant. The droplets tend to align with the flow direction, reducing their deformation and breakup. The typical water channel size used in W/O emulsion studies is between 10 and 1,000 μm (Yi et al., 2022). When the water channel size becomes larger than 1,000 μm, the flow becomes more turbulent and chaotic, and other factors such as contact angle and surfactant concentration may become more critical than water channel size in determining the water droplet size in W/O emulsions. In Fig. 16, the graph shows the water droplet size and oil droplet size at different oil channeling sizes, as per the modeling results. With the increase in water channel size, the droplets are formed earlier, their size is larger and they are also more

distant from each other, which is the reason for the use of a larger volume of water entering the environment. Also, as this parameter increases, the drops from earlier and immediately after entering the oil path. The changes mentioned in Fig. 17 can be seen. In Fig. 18, the graph shows the water droplet size and oil droplet size at different water channeling sizes, as per the modeling results.

4. Conclusions

In this research, by modeling using COMSOL Multiphysics software and validating the results with the laboratory experimental results through T-junction microfluidics, we were able to study different parameters that affect the shape and behavior of water-in-oil (W/O) emulsions, and the main findings of this study are summarized as follows:

1) The IFT between water and oil varies with the salinity of the water. There are two regions of IFT behavior: One where IFT increases with decreasing salinity, and one where IFT decreases with decreasing salinity. This is due to the effects of salt and polar components (for example, asphaltene molecules) on the oil-water interface. The presence of asphaltenes, which are natural surfactants, can decrease the IFT by interacting with both phases. However, at high salinities, the salt effect dominates over the asphaltene effect and increases the IFT. There is an optimal point of salinity where the IFT is the lowest.
2) The IFT, which depends on the salt content, is inversely proportional to the size of the water droplets in W/O emulsions. For the seawater diluted two times (SW#2), the optimal IFT and water droplet size is achieved. The size of water droplets also depends on the rate at which a continuous and dispersed phase flows. Water droplets increase in size as the water flow increases to an unchanging oil flow rate. When the oil flow rate increases at a constant water flow rate, the water droplets become smaller. This is because of the effects of shear rate, Re and We on the droplet deformation and breakup processes.
3) The contact angle between immiscible fluids and walls affects the formation, size, and stability of droplets in an emulsion. A lower contact angle leads to larger water droplets and smaller oil droplets, while a higher contact angle leads to smaller water droplets and larger oil droplets.
4) Oil viscosity significantly impacts the stability and size of water droplets in W/O emulsions. Lower oil viscosity results in smaller water droplets and larger oil droplets, whereas higher oil viscosity produces larger water droplets and smaller oil droplets. The effective viscosity of these emulsions, which measures resistance to flow, is influenced by IFT and droplet size. Effective viscosity is determined by shear stress divided by shear rate and depends on factors like volume fraction, size distribution, shape, and droplet deformation. IFT indirectly affects effective viscosity by altering droplet size and shape. Water droplet size and stability in W/O emulsions are influenced by channel size. Smaller channel sizes result in higher shear rates and Re, promoting droplet breakup, while lower We, decrease droplet coalescence. There are critical channel sizes below which the droplet size does not decrease further but increases slightly, likely due to laminar flow and confinement effects. Other factors such as contact angle and IFT may become more critical than channel size in determining the droplet size in W/O emulsions.

Acknowledgements

This study was a part of Taha Zarin's MSc thesis. The oil samples were provided by the Iranian Offshore Oil Company (IOOC), and we thank them for their contribution.

Conflict of interest

The authors declare no competing interest.

References

Aghajanzadeh, M. R., Ahmadi, P., Sharifi, M., et al. Wettability modification of oil-wet carbonate reservoirs using silica-based nanofluid: An experimental approach. Journal of Petroleum Science and Engineering, 2019, 178: 700-710.

Aghajanzadeh, M. R., Sharifi, M. Stabilizing silica nanoparticles in high saline water by using polyvinylpyrrolidone for reduction of asphaltene precipitation damage under dynamic condition. Chinese Journal of Chemical Engineering, 2019, 27(5): 1021-1029.

Anna, S. L., Bontoux, N., Stone, H. A. Formation of dispersions using "flow focusing" in microchannels. Applied Physics Letters, 2003, 82(3): 364-366.

Battat, S., Weitz, D. A., Whitesides, G. M. Nonlinear phenomena in microfluidics. Chemical Reviews, 2022, 122(7): 6921-6937.

Bera, A., Ojha, K., Kumar, T., et al. Water solubilization capacity, interfacial compositions and thermodynamic parameters of anionic and cationic microemulsions. Colloids and Surfaces A: Physicochemical and Engineering Aspects, 2012, 404: 70-77.

Boniou, V., Schmitt, T., Vié, A. Comparison of interface capturing methods for the simulation of two-phase flow in a unified low-Mach framework. International Journal of Multiphase Flow, 2022, 149: 103957.

Cramer, C., Fischer, P., Windhab, E. J. Drop formation in a co-flowing ambient fluid. Chemical Engineering Science, 2004, 59(15): 3045-3058.

De Menech, M. Modeling of droplet breakup in a microfluidic T-shaped junction with a phase-field model. Physical Review E-Statistical, Nonlinear, and Soft Matter Physics, 2006, 73(3): 031505.

Doryani, H., Malayeri, M. R., Riazi, M. Precipitation and deposition of asphaltene in porous media: Impact of various connate water types. Journal of Molecular Liquids, 2018,

258: 124-132.

Duraiswamy, S., Khan, S. A. Droplet-based microfluidic synthesis of anisotropic metal nanocrystals. Small, 2009, 5(24): 2828-2834.

El-Aooiti, M., de Vries, A., Rousseau, D. Demulsification of water-in-oil emulsions stabilized with glycerol monostearate crystals. Journal of Colloid and Interface Science, 2023, 636: 637-645.

Garstecki, P., Fuerstman, M. J., Stone, H. A., et al. Formation of droplets and bubbles in a microfluidic T-junction-scaling and mechanism of break-up. Lab on a Chip, 2006, 6(3): 437-446.

Gong, C., Towner, J. W. Study of dynamic interfacial tension for demulsification of crude oil emulsions. Paper SPE 65012 Presented at the SPE International Symposium on Oilfield Chemistry, Houston, Texas, 13-16 February, 2001.

Guillot, P., Colin, A. Stability of parallel flows in a microchannel after a T junction. Physical Review E-Statistical, Nonlinear, and Soft Matter Physics, 2005, 72(6): 066301.

Gupta, A., Kumar, R. Flow regime transition at high capillary numbers in a microfluidic T-junction: Viscosity contrast and geometry effect. Physics of Fluids, 2010, 22(12): 122001.

He, K., Lin, Y., Hu, Y., et al. Phase separation features of oil-water parallel flow at hydrophobic and hydrophilic micro-T-junctions. Chemical Engineering Science, 2022, 253: 117520.

Hoang, D. A., Portela, L. M., Kleijn, C. R., et al. Dynamics of droplet breakup in a T-junction. Journal of Fluid Mechanics, 2013, 717: R4.

Ho, T. M., Razzaghi, A., Ramachandran, A., et al. Emulsion characterization via microfluidic devices: A review on interfacial tension and stability to coalescence. Advances in Colloid and Interface Science, 2022, 299: 102541.

Jang, H. K., Hong, S. O., Lee, S. B., et al. Viscosity measurement of non-Newtonian fluids in pressure-driven flows of general geometries based on energy dissipation rate. Journal of Non-Newtonian Fluid Mechanics, 2019, 274: 104204.

Jiang, Y., Wang, C., Zhang, F., et al. Microscopic visualization experimental study on the effect and mechanism of viscosity reducer on emulsification of heavy oil. Energies, 2023, 16(6): 2538.

Kim, J. W., Han, S. H., Choi, Y. H., et al. Recent advances in the microfluidic production of functional microcapsules by multiple-emulsion templating. Lab on a Chip, 2022, 22(12): 2259-2291.

Kousksou, T., Bruel, P., Jamil, A., et al. Energy storage: Applications and challenges. Solar Energy Materials and Solar Cells, 2014, 120: 59-80.

Kovalchuk, N. M., Simmons, M. J. Review of the role of surfactant dynamics in drop microfluidics. Advances in Colloid and Interface Science, 2023, 312: 102844.

Liu, Y., Bai, J., Guo, P., et al. Experimental Study on Water-in-Heavy-Oil Droplets Stability and Viscosity Variations in the Dilution Process of Water-in-Heavy-Oil Emulsions by Light Crude Oil. Energies, 2024, 17(2): 332.

Li, W., Sun, Z., Li, N., et al. Effect of the Weber number on the coalescence of relatively moving droplets in an electric field: A molecular dynamics study. Journal of Molecular Liquids, 2023, 388: 122783.

Lv, Q., Li, J., Guo, P., et al. Effect of Reynolds number on impact force and collision process of a low-velocity droplet colliding with a wall carrying an equal-mass deposited droplet. International Journal of Multiphase Flow, 2023, 163: 104432.

Mahmood, M. N., Nguyen, V., Guo, B. Challenges in mathematical modeling of dynamic mass transfer controlled by capillary and viscous forces in spontaneous fluid imbibition processes. Capillarity, 2024, 11(2): 53-62.

Ma, J., Yao, M., Yang, Y., et al. Comprehensive review on stability and demulsification of unconventional heavy oil-water emulsions. Journal of Molecular Liquids, 2022, 350: 118510.

Mangani, F., Soligo, G., Roccon, A., et al. Influence of density and viscosity on deformation, breakage, and coalescence of bubbles in turbulence. Physical Review Fluids, 2022, 7(5): 053601.

Ming, L., Wu, H., Liu, A., et al. Evolution and critical roles of particle properties in Pickering emulsion: A review. Journal of Molecular Liquids, 2023, 388: 122775.

Mohammadi, M., Shafiei, M., Zarin, T., et al. Application of smoothed particle hydrodynamics for modeling of multiphase fluid flow in non-uniform porous media. Industrial & Engineering Chemistry Research, 2023, 62(33): 13181-13200.

Nguyen, B. T., Nicolai, T., Benyahia, L. Stabilization of water-in-water emulsions by addition of protein particles. Langmuir, 2013, 29(34): 10658-10664.

Ntente, C., Strekla, A., Iatridi, Z., et al. Polymer-coated nanoparticles and pickering emulsions as agents for enhanced oil recovery: Basic studies using a porous medium model. Energies, 2023, 16(24): 8043.

Osher, S., Fedkiw, R. P. Level set methods: an overview and some recent results. Journal of Computational Physics, 2001, 169(2): 463-502.

Persson, P. O. The level set Method lecture notes. Massachusetts Institute of Technology Cambridge, 2013.

Rahimi, A., Honarvar, B., Safari, M. The role of salinity and aging time on carbonate reservoir in low salinity seawater and smart seawater flooding. Journal of Petroleum Science and Engineering, 2020, 187: 106739.

Rezaei, N., Firoozabadi, A. Macro-and microscale waterflooding performances of crudes which form w/o emulsions upon mixing with brines. Energy & Fuels, 2014, 28(3): 2092-2103.

Romero, P. A., Abate, A. R. Flow focusing geometry generates droplets through a plug and squeeze mechanism. Lab on a Chip, 2012, 12(24): 5130-5132.

Salehpour, M., Sakhaei, Z., Salehinezhad, R., et al. Contribution of water-in-oil emulsion formation and pressure fluctuations to low salinity waterflooding of asphaltic oils: A pore-scale perspective. Journal of Petroleum Science and Engineering, 2021, 203: 108597.

Sang, L., Hong, Y., Wang, F. Investigation of viscosity ef-

fect on droplet formation in T-shaped microchannels by numerical and analytical methods. Microfluidics and Nanofluidics, 2009, 6: 621-635.

Sattari, A., Hanafizadeh, P., Hoorfar, M. Multiphase flow in microfluidics: From droplets and bubbles to the encapsulated structures. Advances in Colloid and Interface Science, 2020, 282: 102208.

Shende, T., Niasar, V. J., Babaei, M. Effective viscosity and Reynolds number of non-Newtonian fluids using Meter model. Rheologica Acta, 2021, 60(1): 11-21.

Soo, H., Radke, C. J. Flow mechanism of dilute, stable emulsions in porous media. Industrial & Engineering Chemistry Fundamentals, 1984, 23(3): 342-347.

Sun, J., Li, Z., Furtado, F., et al. A microfluidic study of transient flow states in permeable media using fluorescent particle image velocimetry. Capillarity, 2021, 4(4): 76-86.

Tagavifar, M., Xu, K., Jang, S. H., et al. Spontaneous and flow-driven interfacial phase change: dynamics of microemulsion formation at the pore scale. Langmuir, 2017, 33(45): 13077-13086.

Tangparitkul, S., Sukee, A., Jiang, J., et al. Role of interfacial tension on wettability-controlled fluid displacement in porous rock: A capillary-dominated flow and how to control it. Capillarity, 2023, 9(3): 55-64.

Tan, Y. C., Fisher, J. S., Lee, A. I., et al. Design of microfluidic channel geometries for the control of droplet volume, chemical concentration, and sorting. Lab on a Chip, 2004, 4(4): 292-298.

Thai, N. T., Xuan, C. T., Thanh, P. D., et al. Formation of microdroplet in T-junction microfluidic system: Experiment and simulation. Communications in Physics, 2018, 28(3): 225-235.

Thorsen, T., Roberts, R. W., Arnold, F. H., et al. Dynamic pattern formation in a vesicle-generating microfluidic device. Physical Review Letters, 2001, 86(18): 4163.

Unsal, E., Broens, M., Armstrong, R. T. Pore scale dynamics of microemulsion formation. Langmuir, 2016, 32(28): 7096-7108.

Van der Graaf, S., Nisisako, T., Schroën, C., et al. Lattice Boltzmann simulations of droplet formation in a T-shaped microchannel. Langmuir, 2006, 22(9): 4144-4152.

Wang, H., Li, J., Fan, C., et al. Thermal kinetics of coal spontaneous combustion based on multiphase fully coupled fluid-mechanical porous media model. Natural Resources Research, 2022, 31(5): 2819-2837.

Wang, M., Kong, C., Liang, Q., et al. Numerical simulations of wall contact angle effects on droplet size during step emulsification. RSC Advances, 2018, 8(58): 33042-33047.

Ward, T., Faivre, M., Abkarian, M., et al. Microfluidic flow focusing: Drop size and scaling in pressure versus flow-rate-driven pumping. Electrophoresis, 2005, 26(19): 3716-3724.

Xiao, Y., He, Y., Zheng, J., et al. Modeling of two-phase flow in heterogeneous wet porous media. Capillarity, 2022, 5(3): 41-50.

Xu, J. H., Li, S. W., Tan, J., et al. Preparation of highly monodisperse droplet in a T-junction microfluidic device. AIChE Journal, 2006, 52(9): 3005-3010.

Yang, Y., Peng, W., Zhang, H., et al. The oil/water interfacial behavior of microgels used for enhancing oil recovery: A comparative study on microgel powder and microgel emulsion. Colloids and Surfaces A: Physicochemical and Engineering Aspects, 2022, 632: 127731.

Yeh, S. L., Koshani, R., Sheikhi, A. Colloidal aspects of calcium carbonate scaling in water-in-oil emulsions: A fundamental study using droplet-based microfluidics. Journal of Colloid and Interface Science, 2023, 633: 536-545.

Yi, L., Wang, C., van Vuren, T., et al. Physical mechanisms for droplet size and effective viscosity asymmetries in turbulent emulsions. Journal of Fluid Mechanics, 2022, 951: A39.

Zarin, T., Sufali, A., Ghaedi, M. Systematic comparison of advanced models of two-and three-parameter equations to model the imbibition recovery profiles in naturally fractured reservoirs. Journal of Petroleum Exploration and Production Technology, 2023, 13(10): 2125-2137.

Zhang, B., Li, J., Guo, P., et al. Experimental studies on the effect of Reynolds and Weber numbers on the impact forces of low-speed droplets colliding with a solid surface. Experiments in Fluids, 2017, 58: 1-12.

Zhang, J., Wang, X., Liang, Q., et al. Demulsification law of polyether demulsifier for W/O crude oil emulsion containing hydrophobically modified polyacrylamide in water. Journal of Molecular Liquids, 2024, 394: 123805.